Key Points:
- Here we have reported the experimental evidence for a thermally stable phase of $CaCO_3$, $CaCO_3$-VII, at the top lower mantle
- $CaCO_3$-VII reacts with stishovite at depths of 700–1,000 km to form $CaSiO_3$-pervoskite and release CO_2 to the surrounding mantle
- $CaCO_3$-VII is an important carbon carrier at the Earth's topmost lower mantle

Correspondence to:
Z. Mao,
zhumao@ustc.edu.cn

New High-Pressure Phase of $CaCO_3$ at the Topmost Lower Mantle: Implication for the Deep-Mantle Carbon Transportation

Xinyang Li[1] (ID), Zhigang Zhang[2,3] (ID), Jung-Fu Lin[4] (ID), Huaiwei Ni[1] (ID), Vitali B. Prakapenka[5] (ID), and Zhu Mao[1] (ID)

[1]Laboratory of Seismology and Physics of Earth's Interior, School of Earth and Planetary Sciences, University of Science and Technology of China, Hefei, China, [2]Key Laboratory of Earth and Planetary Physics, Institute of Geology and Geophysics, Chinese Academy of Sciences, Beijing, China, [3]College of Earth Science, University of Chinese Academy of Sciences, Beijing, China, [4]Department of Geological Sciences, Jackson School of Geosciences, The University of Texas at Austin, Austin, TX, USA, [5]Center for Advanced Radiation Sources, University of Chicago, Chicago, IL, USA

Abstract In this study, we have investigated the stability of $CaCO_3$ at high pressures and temperatures using synchrotron X-ray diffraction in laser-heated diamond anvil cells. Our experimental results have shown that $CaCO_3$ in the aragonite structure transforms into $CaCO_3$-VII ($P2_1/c$) at 27 GPa and 1,500 K with a negative Clapeyron slope of $-4.3(9)$ MPa/K. $CaCO_3$-VII is stable between 23 and 38 GPa at 2,300 K and transforms into post-aragonite at 42 GPa and 1,400 K. Furthermore, it reacts with stishovite, an abundant form of SiO_2 in subducted oceanic crust, forming $CaSiO_3$-perovskite. The occurrence of $CaSiO_3$-perovskite via the reaction of $CaCO_3$-VII and stishovite provides an explanation for the observation of the high concentrations of $CaSiO_3$-perovskite and some amount of $CaCO_3$ in deep-mantle inclusions. $CaCO_3$-VII is thus an important carbon-bearing phase at the topmost lower mantle and may provide necessary carbon to produce deep-mantle diamonds.

1. Introduction

Petrologists have recently found more evidence for the formation of deep diamonds at the topmost lower mantle, suggesting the transportation of surface carbon to the Earth's deep interior (Brenker et al., 2007; Burnham et al., 2016; Kaminsky et al., 2009, 2016; Shirey et al., 2013; Smith et al., 2016; Wirth et al., 2009). Carbonates, including calcite ($CaCO_3$), magnesite ($MgCO_3$), and dolomite ($CaMg(CO_3)_2$, are believed to be one of the most important carriers to transport surface carbon to the Earth's mantle. Notably, some deep diamonds expected from the topmost lower mantle capture carbonates, such as $CaCO_3$, as inclusions together with very high abundance of $CaSiO_3$ perovskite than what is expected from typical mantle mineralogy (Brenker et al., 2007; Kaminsky et al., 2009, 2016; Wirth et al., 2009). Although a recent experimental study has shown that melting of the carbonated oceanic crust at depth of 300–700 km could become a barrier for the transportation of carbon to the deeper mantle, some carbonates in the cold slab surface may survive at least to the topmost lower mantle and are thus the potential carriers to transport carbon to the Earth's deep mantle (Brenker et al., 2007; Kaminsky et al., 2009, 2016; Thomson et al., 2016; Wirth et al., 2009).

Among various carbonates, $CaCO_3$ is most abundant on Earth and mainly crystallizes in the form of calcite at the Earth's surface. Through hydrothermal metasomatism, a significant amount of $CaCO_3$ in the form of calcite enters the oceanic crust to form carbonate-bearing altered oceanic basalt (Alt & Teagle, 1999; Jarrard, 2003; Kelemen & Manning, 2015). Analysis of the inclusions in deep diamonds has revealed evidence of the transportation of $CaCO_3$ to depths of at least the topmost lower mantle via sinking slabs (Brenker et al., 2007; Kaminsky et al., 2009, 2016; Wirth et al., 2009). Previous studies have further shown that $CaCO_3$ undergoes a series of phase transitions at high pressures (Catalli & Williams, 2005; Gavryushkin et al., 2017; Lobanov et al., 2017; Oganov et al., 2008, 2006; Ono et al., 2005; Pickard & Needs, 2015; Smyth & Ahrens, 1997; Suito et al., 2001). At 300 K, $CaCO_3$ in calcite structure will transform into $CaCO_3$-III at 2.5 GPa, whereas $CaCO_3$-III transforms into $CaCO_3$-VI at 15 GPa (Merlini et al., 2012). Although previous experimental and theoretical studies have shown that $CaCO_3$ crystallizes in the form of aragonite at pressure-temperature conditions of the topmost lower mantle, a new phase
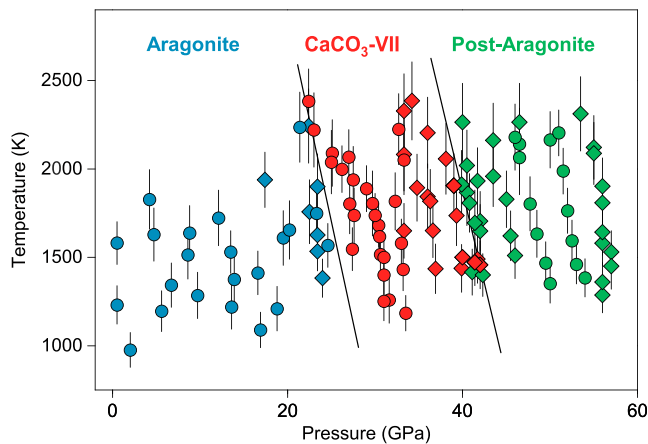
Figure 1. Phase diagram of CaCO$_3$ at high pressures and temperatures. Blue: aragonite; red: CaCO$_3$-VII; green: post-aragonite; circles: using NaCl as the pressure medium; diamonds: using KCl as the pressure medium. The black lines indicate the phase boundary between aragonite and CaCO$_3$-VII and between CaCO$_3$-VII and postaragonite.

Figure 2. X-ray diffraction patterns of CaCO$_3$ at high pressures and temperatures. (a) Diffraction pattern of aragonite at 29 GPa and 300 K, CaCO$_3$-VII at 31 GPa and 1,570 K, and CaCO$_3$-VII at 32 GPa and 300 K. (b) Results from full-profile Rietveld refinement of CaCO$_3$-VII at 32 GPa and 300 K, showing CaCO$_3$-VII in a $P2_1/c$ structure. Red line: refinement results; black cross: collected data. The X-ray wavelength is 0.3344 Å.

between 32 and 48 GPa with a space group of $P2_1/c$ has been predicted by a recent theoretical study (Oganov et al., 2006, 2008; Ono et al., 2005; Pickard & Needs, 2015; Santillan & Williams, 2004; Suito et al., 2001). A recent experimental study reported two new phases of CaCO$_3$, named aragonite-II and CaCO$_3$-VII, between 30 and 50 GPa at high temperatures (Gavryushkin et al., 2017). Yet neither aragonite-II nor CaCO$_3$-VII was observed to be a pure phase at high pressures and temperatures (Gavryushkin et al., 2017). Aragonite-II coexists with aragonite and CaCO$_3$-VII at ~26 GPa between 1,400 K and 2,400 K, while CaCO$_3$-VII coexists with postaragonite between 40 and 50 GPa at 1,200–2,200 K (Gavryushkin et al., 2017). Due to limited experimental data points and without using pressure medium in some experimental runs, the phase stability of both aragonite-II and CaCO$_3$-VII is highly uncertain in the previous study (Gavryushkin et al., 2017). The high pressure-temperature stability of CaCO$_3$ thus needs further investigation.

In addition, analysis of the mineralogy of deep-mantle diamond inclusions further suggests that carbonates could potentially react with silicates in subducted slabs and provide carbon-rich fluids for the formation of diamonds (Biellmann et al., 1993; Hammouda, 2003; Kushiro et al., 1975; Maeda et al., 2017). However, experimental data on the phase stability of the high-pressure phase of CaCO$_3$ coexisting with other minerals in the subducted slabs at relevant pressure and temperature conditions at the top of the lower mantle are lacking. In this study, we thus investigated the phase stability of CaCO$_3$ with coexisting minerals in slabs under the relevant pressure and temperature conditions of the topmost lower mantle using synchrotron X-ray diffraction (XRD) in laser-heated diamond anvils. Our experimental results are crucial for understanding the deep carbon transportation and the distinct mineralogy of deep diamond inclusions.

2. Experiments

The crystal structure and chemical composition of natural calcite (CaCO$_3$) from Guizhou Province of China were determined by XRD and electron microprobe at surface conditions at the Material Center of the University of Science and Technology of China, respectively. The natural calcite sample contains minimum amount of K within the measurement error of the electron microprobe. The calcite sample was thus considered with a composition of CaCO$_3$. To study the high-pressure phase transition of CaCO$_3$, the powder was mixed with 5 wt % Pt, which acted as the pressure calibrant and laser absorber (Fei et al., 2007). The CaCO$_3$ + Pt mixture was pressed into 15–20 μm thick disks and then loaded into two symmetric diamond anvil cells. NaCl was used as the pressure medium in one cell, while KCl was used in the other cell. Re was used as the gasket material. To investigate the phase stability of CaCO$_3$, the CaCO$_3$ powder was also mixed with SiO$_2$ powder in equal molar proportions. The CaCO$_3$ + SiO$_2$ powder was then mixed with 5 wt.% Pt, which acted as a pressure calibrant and laser absorber. We prepared four samples to study the phase stability of CaCO$_3$ with SiO$_2$. Two cells used NaCl that had been dried overnight as the pressure medium, while the other two used KCl as the pressure medium.

We have conducted high pressure-temperature synchrotron XRD measurements on the phase transition of CaCO$_3$ up to the topmost lower
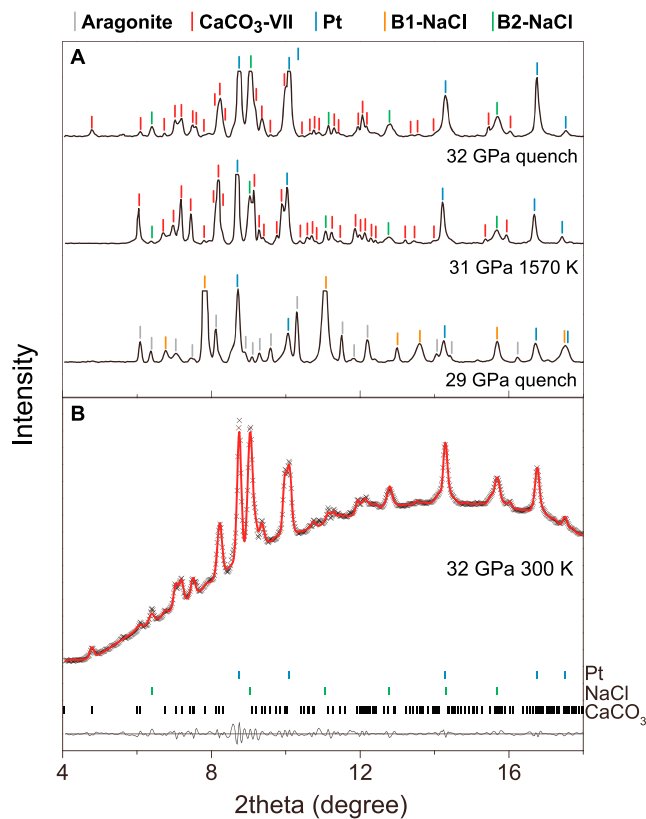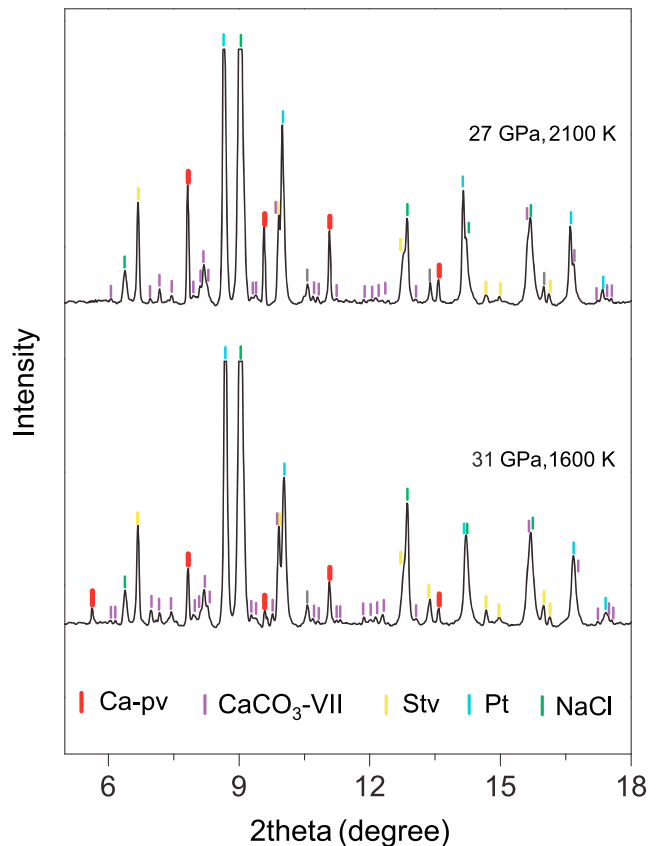
Figure 3. Representative X-ray diffraction patterns for the reaction between CaCO₃-VII and SiO₂. Patterns were collected at 30.5 GPa and 1,600 K and at 27 GPa and 2,100 K, respectively. Stv: stishovite; Ca-Pv: CaSiO₃-perovskite.

mantle conditions. Six runs of the experiments were performed between 1,000 K and 2,400 K at pressures up to 60 GPa in laser-heated diamond anvil cells at the GeoSoilEnviroCARS (GSECARS) of the Advanced Photon Source (APS), Argonne National Laboratory. In each heating cycle, we always heated a fresh spot and collected the XRD patterns at a temperature step of 100–200 K. Following the Graybody approximation, the collected thermal radiation spectrum was fitted using the Planck radiation function to determine the temperature. The uncertainty of the temperature is about ±150 K below 2,000 K and ±200 K above 2,000 K. The XRD patterns were collected using a 165MAR-CCD detector with an X-ray beam focused down to 3×4 μm and an energy of 37 keV.

3. Results and Discussion

At pressures of less than 25 GPa, the starting carbonate transitions into aragonite (space group: *Pnma*) upon laser heating to 1,000 K (Figures 1 and 2). The diffraction pattern is well explained by the presence of aragonite, Pt, and pressure medium NaCl (or KCl) (Figure 2). In the following heating run at a higher pressure, the increase of temperature immediately induces the presence of ~30 new diffraction peaks (Figure 2). These new peaks are not associated with the decomposition products of CaCO₃ such as CaO or high-pressure polymorphs of CO₂ (Datchi et al., 2006, 2012; Deng et al., 2007), indicating the phase transition of CaCO₃ to a new structure without chemical dissociation. Comparison of the diffraction lines of this new phase with that of the known CaCO₃ high-pressure phases shows that the new phase is not CaCO₃-VI, post-aragonite, or any multiphase (Figure S1) (Merlini et al., 2012; Oganov et al., 2006; Ono et al., 2005). The phase has the same structure with CaCO₃-VII in Gavryushkin et al. (2017). The negative Clapeyron slope of the phase boundary between aragonite

and CaCO₃-VII, as well as that of the phase boundary between CaCO₃-VII and post-aragonite, is −4.3(9) MPa/K, which is well constrained by our dense data points. CaCO₃-VII is stable at 23 GPa (720 km depth) up to 2,300 K, which can also be quenched to 300 K at high pressures (Figure 2). Above 42 GPa and 1,400 K, post-aragonite becomes the stable structure of CaCO₃ (Figure 1). The diffraction pattern of CaCO₃-VII can be characterized as a monoclinic cell with a space group of $P2_1/c$, which is consistent with the first principles predictions based on density functional theory (Pickard & Needs, 2015). We further performed the Rietveld full-profile refinements on the diffraction patterns and obtained the lattice parameters of $a = 4.798(4)$ Å, $b = 3.356(2)$ Å, $c = 10.981(6)$ Å, and $\beta = 103.6^o(1)$ for CaCO₃-VII (Toby, 2001). The Ca-O coordination number of the new phase is 9, the same as aragonite. Nonetheless, compared with the structures of aragonite and post-aragonite, the carbonate ions in this new phase are distorted by unequal C–O bond lengths and a nonplanar geometry (Figure S2 and Table S1) (Oganov et al., 2006; Ono et al., 2005; Pickard & Needs, 2015). The phase transition from aragonite to CaCO₃-VII results in a ~1.7% reduction in the volume of CaCO₃ at 300 K (Figure S3). Further transition to post-aragonite lowers the volume of CaCO₃ by ~3.7% (Figure S3).

We compared our experimental results with previous studies in Figure S4. The phase transitions from aragonite to CaCO₃-VII and then to post-aragonite were predicted by a theoretical study at 0 K (Pickard & Needs, 2015). Here we combined the theoretical results at 0 K with the experimentally determined Clapeyron slope from this study to extrapolate the theoretical phase boundary to high temperatures (Figure S4) (Pickard & Needs, 2015). The calculated phase boundaries between aragonite and CaCO₃-VII and between CaCO₃-VII and post-aragonite are in an excellent agreement with our experimental results (Pickard & Needs, 2015). Gavryushkin et al. (2017) performed both high pressure-temperature experiments and theoretical calculations but yield conflicting results. The predicted phase transition between CaCO₃-VII and post-aragonite at a given temperature using density function theory occurs at a much lower pressure than their

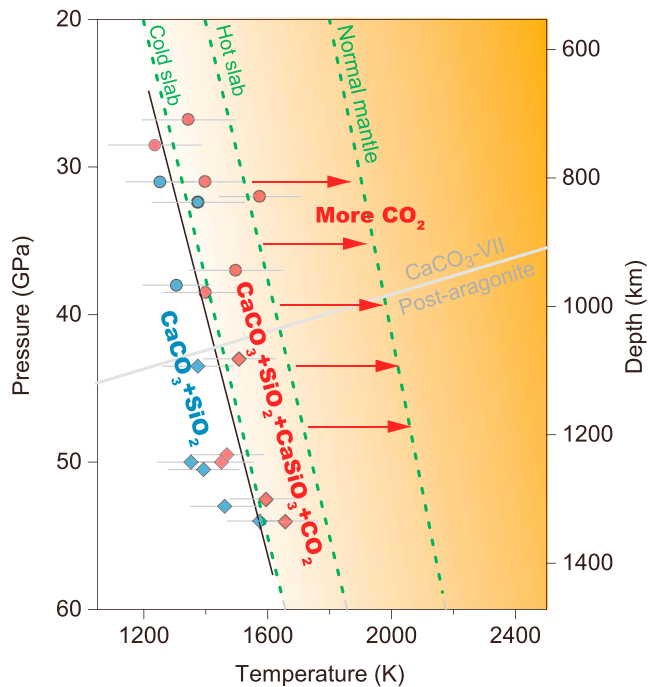**Figure 4.** Phase stability of $CaCO_3$-VII in the presence of SiO_2.; blue: $CaCO_3$ does not react with SiO_2; red: $CaCO_3$ reacts with Stv to release CO_2 to the mantle; circles: $CaCO_3$ in $CaCO_3$-VII structure; diamonds: $CaCO_3$ in postaragonite structure; grey solid line: phase boundary between $CaCO_3$-VII (postaragonite) + SiO_2 and $CaCO_3$-VII (postaragonite) + SiO_2 + $CaSiO_3$ + CO_2; green dashed lines: geotherms for the normal mantle, hot slab, and cold slabs (Akaogi et al., 1989; Litasov & Ohtani, 2003).

experimental results and our observation. In contrast, the experimental phase boundary between $CaCO_3$-VII and post-aragonite in Gavryushkin et al. (2017) is ~7 GPa higher than our experimental results at a given temperature. The difference in the transition pressure could be caused by the use of different pressure calibrant materials (Gavryushkin et al., 2017). The phase boundary determined without using any pressure medium may also have large uncertainties (Gavryushkin et al., 2017). In addition, we did not observe the presence of aragonite-II reported in Gavryushkin et al. (2017) at high pressure-temperature conditions. It is worth noting that aragonite-II was not a pure phase at high pressure-temperature (Gavryushkin et al., 2017). It was observed to coexist with aragonite and $CaCO_3$-VII at high pressure-temperature and characterized by limited XRD peaks. We suspect that aragonite-II observed in the previous study could be a result of contamination during laser heating at high pressures without using pressure medium (Gavryushkin et al., 2017). In this study, two separate high pressure-temperature XRD experiments using either NaCl or KCl as the pressure medium have confirmed that $CaCO_3$-VII is stable up to 2,300 K between 23 and 38 GPa (Figures 1 and 2). Increasing heating time up to 30 min at various pressures above 1,200 K did not cause observable changes in the collected diffraction pattern. Decomposition or further phase transition of $CaCO_3$-VII at high temperatures was not observed. Dense experimental data points also allow us to well constrain the phase boundary among aragonite, $CaCO_3$-VII, and postaragonite. We thus believe that $CaCO_3$-VII is a stable high-pressure phase of $CaCO_3$ at high temperatures.

We further found that $CaCO_3$-VII can react with stishovite-SiO_2 (Stv) to produce Ca-Pv under above pressure and temperature conditions. The reaction between $CaCO_3$-VII and Stv is evidenced by the presence of cubic Ca-Pv in our high pressure-temperature XRD patterns collected at ~30 GPa and temperatures above 1,500 K (Figures 3, S5, and S6). The formation of Ca-Pv can be easily identified by the clear continuous diffraction rings in the analysis of the measured XRD patterns (Figure S6). The formation of Ca-Pv also suggests that CO_2 is released by the $CaCO_3$-VII-Stv reaction. The reaction can be written as follows:

$$CaCO_3 + SiO_2 \rightarrow CaSiO_3 + CO_2$$
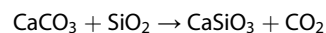
No diffraction peaks associated with CO_2 are observed in our XRD patterns, potentially due to the very weak X-ray scattering and possible disordered nature of CO_2 phase under these conditions (Datchi et al., 2006; Datchi et al., 2012). The intensity of the Ca-Pv peaks increases with increasing temperature with the gradual disappearance of $CaCO_3$ and Stv, showing that the reaction between the $CaCO_3$-VII phase of $CaCO_3$ and Stv can be enhanced by higher temperatures and result in the release of more CO_2 to the surrounding mantle (Figures 3 and 4). In addition, our results also show that post-aragonite will also react with Stv at higher pressures (Figures S7 and S8).

4. Geophysical Implications

The experimental results above have profound implications for the carbon circulation at the topmost lower mantle. As the most abundant natural carbonate, $CaCO_3$, mainly in the form of calcite, is transported to the Earth's interior via sinking subducted slabs of calcite-rich oceanic crust. Some $CaCO_3$ that transforms from calcite to aragonite will likely react with mantle pyroxene and/or olivine during the subduction process, whereas a large amount of $CaCO_3$ may become unstable in slab melting and cannot be transported to the deeper depth (Biellmann et al., 1993; Stagno et al., 2015; Thomson et al., 2016). However, some $CaCO_3$ in cold slabs will likely survive, depending on the local mineral proportions and pressure-temperature-compositional environments of the slab (Brenker et al., 2007; Kaminsky et al., 2009, 2016; Thomson et al., 2016; Wirth et al., 2009). In addition, some $CaCO_3$ in the slab could also be produced through dolomite-pyroxene

and/or dolomite-olivine reactions (Biellmann et al., 1993; Hammouda, 2003; Kushiro et al., 1975; Martinez et al., 1996; Shirasaka et al., 2002). The residual $CaCO_3$ could thus be present in the form of $CaCO_3$-VII at the topmost lower mantle, and some of them could be captured as inclusions in diamonds as shown in recent petrological studies (Brenker et al., 2007; Kaminsky et al., 2009, 2016; Wirth et al., 2009). $CaCO_3$-VII is thus a potential carbon-bearing phase in this region.

Even in cold slabs, our results show that $CaCO_3$-VII will react with Stv, which is an abundant mineral in the mid-ocean ridge basalt, possibly releasing CO_2 to the surrounding mantle (Figure 4). It is worth noting that similar reaction between aragonite and Stv to form Ca-Pv may also occur at high pressures and temperatures, but future experiments will be needed to validate this hypothesis. The residual aragonite will transform into $CaCO_3$-VII, which may be captured by diamonds as inclusions or continually react with Stv (Brenker et al., 2007; Kaminsky et al., 2009, 2016; Wirth et al., 2009). The CO_2 released by the $CaCO_3$-VII-Stv reaction, together with the possible presence of water, will lower the melting temperature likely leading to the formation of the C-O-H-bearing fluid or melt needed for the growth of diamonds (Dasgupta & Hirschmann, 2006; Litasov & Ohtani, 2009). The local abundance of Ca-Pv produced by the $CaCO_3$-VII-Stv reaction will be higher than that of the normal mantle (Burnham et al., 2016). This observation could explain why the abundance of Ca-Pv in some deep diamonds is higher than what is expected from typical mantle mineralogy (Burnham et al., 2016; Walter et al., 2008) and why ferropericlase is absent from recently found deep diamonds (Smith et al., 2016). Meanwhile, the residual $CaCO_3$ from the $CaCO_3$-VII-Stv reaction can be captured by diamonds as inclusions or transformed into post-aragonite, thereby becoming the carbon-bearing phase responsible for the transport of carbon to even deeper depths (Brenker et al., 2007; Kaminsky et al., 2016; Wirth et al., 2009). However, the residual $CaCO_3$ after the $CaCO_3$-VII-Stv reaction could be limited. Magnesite ($MgCO_3$), the potential reaction product between dolomite (and/or $CaCO_3$) and mantle enstatite (and/or olivine), is likely to be the major phase responsible for delivering carbon to the middle and bottom of the lower mantle for the formation of superdeep diamonds (Maeda et al., 2017; Walter et al., 2008). As a result, the $CaCO_3$-VII phase of $CaCO_3$ is an important carbon bearing phase at the topmost lower mantle and a crucial source for generating the CO_2-enriched fluid environment. These findings improve the understanding of the deep carbon circulation and the compositions of some deep diamond inclusions."

Reference

Akaogi, M., Ito, E., & Navrotsky, A. (1989). Olivine-modified spinel-spinel transitions in the system Mg_2SiO_4-Fe_2SiO_4: Calorimetric measurements, thermochemical calculation, and geophysical application. *Journal of Geophysical Research*, *94*(B11), 15,671–15,685. https://doi.org/10.1029/JB094iB11p15671

Alt, J. C., & Teagle, D. A. H. (1999). The uptake of carbon during alteration of ocean crust. *Geochimica et Cosmochimica Acta*, *63*(10), 1527–1535. https://doi.org/10.1016/S0016-7037(99)00123-4

Biellmann, C., Gillet, P., Guyot, F., Peyronneau, J., & Reynard, B. (1993). Experimental evidence for carbonate stability in the Earth's lower mantle. *Earth and Planetary Science Letters*, *118*(1-4), 31–41. https://doi.org/10.1016/0012-821X(93)90157-5

Brenker, F. E., Vollmer, C., Vincze, L., Vekemans, B., Szymanski, A., Janssens, K., et al. (2007). Carbonates from the lower part of transition zone or even the lower mantle. *Earth and Planetary Science Letters*, *260*(1-2), 1–9. https://doi.org/10.1016/j.epsl.2007.02.038

Burnham, A. D., Bulanova, G. P., Smith, C. B., Whitehead, S. C., Kohn, S. C., Gobbo, L., & Walter, M. J. (2016). Diamonds from the Machado River alluvial deposit, Rondonia, Brazil, derived from both lithospheric and sublithospheric mantle. *Lithos*, *265*, 199–213. https://doi.org/10.1016/j.lithos.2016.05.022

Catalli, K., & Williams, Q. (2005). A high-pressure phase transition of calcite-III. *American Mineralogist*, *90*(10), 1679–1682. https://doi.org/10.2138/am.2005.1954

Dasgupta, R., & Hirschmann, M. M. (2006). Melting in the Earth's deep upper mantle caused by carbon dioxide. *Nature*, *440*(7084), 659–662. https://doi.org/10.1038/nature04612

Datchi, F., Giordano, V. M., Munsch, P., & Saitta, A. M. (2009). Structure of carbon dioxide phase IV: Breakdown of the intermediate bonding state scenario. *Physical Review Letters*, *103*(18). https://doi.org/10.1103/Physrevlett.103.185701

Datchi, F., Mallick, B., Salamat, A., & Ninet, S. (2012). Structure of polymeric carbon dioxide CO_2-V. *Physical Review Letters*, *108*(12). https://doi.org/10.1103/Physrevlett.108.125701

Deng, Y., Jia, O. H., Chen, X. R., & Zhu, J. (2007). Phase transition and elastic constants of CaO from first-principle calculations. *Physica B*, *392*(1-2), 229–232. https://doi.org/10.1016/j.physb.2006.11.023

Fei, Y. W., Ricolleau, A., Frank, M., Mibe, K., Shen, G. Y., & Prakapenka, V. (2007). Toward an internally consistent pressure scale. *Proceedings of the National Academy of Sciences of the United States of America*, *104*(22), 9182–9186. https://doi.org/10.1073/pnas.0609013104

Gavryushkin, P. N., Martirosyan, N. S., Inerbaev, T. M., Popov, Z. I., Rashchenko, S. V., Likhacheva, A. Y., et al. (2017). Aragonite-II and $CaCO_3$-VII—New high pressure high-temperature polymorphs of $CaCO_3$. *Crystal Growth & Design*, *17*(12), 6291–6296. https://doi.org/10.1021/acs.cgd.7b00977

Hammouda, T. (2003). High-pressure melting of carbonated eclogite and experimental constraints on carbon recycling and storage in the mantle. *Earth and Planetary Science Letters*, *214*(1-2), 357–368. https://doi.org/10.1016/S0012-821X(03)00361-3

Jarrard, R. D. (2003). Subduction fluxes of water, carbon dioxide, chlorine, and potassium. *Geochemistry, Geophysics, Geosystems*, *4*(5), 8905. https://doi.org/10.1029/2002GC000392

Kaminsky, F., Matzel, J., Jacobsen, B., Hutcheon, I., & Wirth, R. (2016). Isotopic fractionation of oxygen and carbon in decomposed lower-mantle inclusions in diamond. *Mineralogy and Petrology*, *110*(2-3), 379–385. https://doi.org/10.1007/s00710-015-0401-7

Kaminsky, F., Wirth, R., Matsyuk, S., Schreiber, A., & Thomas, R. (2009). Nyerereite and nahcolite inclusions in diamond: Evidence for lower-mantle carbonatitic magmas. *Mineralogical Magazine*, *73*(5), 797–816. https://doi.org/10.1180/minmag.2009.073.5.797

Kelemen, P. B., & Manning, C. E. (2015). Reevaluating carbon fluxes in subduction zones, what goes down, mostly comes up. *Proceedings of the National Academy of Sciences of the United States of America*, *112*(30), E3997–E4006. https://doi.org/10.1073/pnas.1507889112

Kushiro, I., Satake, H., & Akimoto, S. (1975). Carbonate-silicate reactions at high-pressures and possible presence of dolomite and magnesite in upper mantle. *Earth and Planetary Science Letters*, *28*(2), 116–120. https://doi.org/10.1016/0012-821X(75)90218-6

Litasov, K. D., & Ohtani, E. (2003). Stability of various hydrous phases in CMAS pyrolite-H_2O system up to 25 GPa. *Physics and Chemistry of Minerals*, *30*(3), 147–156. https://doi.org/10.1007/s00269-003-0301-y

Litasov, K. D., & Ohtani, E. (2009). Phase relations in the peridotite-carbonate-chloride system at 7.0-16.5 GPa and the role of chlorides in the origin of kimberlite and diamond. *Chemical Geology*, *262*(1-2), 29–41. https://doi.org/10.1016/j.chemgeo.2008.12.027

Lobanov, S. S., Dong, X., Martirosyan, N. S., Samtsevich, A. I., Stevanovic, V., Gavryushkin, P. N., et al. (2017). Raman spectroscopy and X-ray diffraction of sp3-$CaCO_3$ at lower mantle pressures. *Physical Review B*, *96*(10), 104101. https://doi.org/10.1103/PhysRevB.96.104101

Maeda, F., Ohtani, E., Kamada, S., Sakamaki, T., Hirao, N., & Ohishi, Y. (2017). Diamond formation in the deep lower mantle: A high-pressure reaction of $MgCO_3$ and SiO_2. *Scientific Reports*, *7*. https://doi.org/10.1038/Srep40602

Martinez, I., Zhang, J. Z., & Reeder, R. J. (1996). In situ X-ray diffraction of aragonite and dolomite at high pressure and high temperature: Evidence for dolomite breakdown to aragonite and magnesite. *American Mineralogist*, *81*(5-6), 611–624. https://doi.org/10.2138/am-1996-5-608

Merlini, M., Hanfland, M., & Crichton, W. A. (2012). $CaCO_3$-III and $CaCO_3$-VI, high-pressure polymorphs of calcite: Possible host structures for carbon in the Earth's mantle. *Earth and Planetary Science Letters*, *333*, 265–271.

Oganov, A. R., Glass, C. W., & Ono, S. (2006). High-pressure phases of $CaCO_3$: Crystal structure prediction and experiment. *Earth and Planetary Science Letters*, *241*(1-2), 95–103. https://doi.org/10.1016/j.epsl.2005.10.014

Oganov, A. R., Ono, S., Ma, Y. M., Glass, C. W., & Garcia, A. (2008). Novel high-pressure structures of $MgCO_3$, $CaCO_3$ and CO_2 and their role in Earth's lower mantle. *Earth and Planetary Science Letters*, *273*(1-2), 38–47. https://doi.org/10.1016/j.epsl.2008.06.005

Ono, S., Kikegawa, T., Ohishi, Y., & Tsuchiya, J. (2005). Post-aragonite phase transformation in $CaCO_3$ at 40 GPa. *American Mineralogist*, *90*(4), 667–671. https://doi.org/10.2138/am.2005.1610

Pickard, C. J., & Needs, R. J. (2015). Structures and stability of calcium and magnesium carbonates at mantle pressures. *Physical Review B*, *91*(10), 104101. https://doi.org/10.1103/Physrevb.91.104101

Santillan, J., & Williams, Q. (2004). A high pressure X-ray diffraction study of aragonite and the post-aragonite phase transition in $CaCO_3$. *American Mineralogist*, *89*(8-9), 1348–1352. https://doi.org/10.2138/am-2004-8-925

Shirasaka, M., Takahashi, E., Nishihara, Y., Matsukage, K., & Kikegawa, T. (2002). In situ X-ray observation of the reaction dolomite = aragonite plus magnesite at 900–1300 K. *American Mineralogist*, *87*(7), 922–930. https://doi.org/10.2138/am-2002-0715

Shirey, S. B., Cartigny, P., Frost, D. J., Keshav, S., Nestola, F., Nimis, P., et al. (2013). Diamonds and the geology of mantle carbon. *Reviews in Mineralogy and Geochemistry*, *75*(1), 355–421. https://doi.org/10.2138/rmg.2013.75.12

Smith, E. M., Shirey, S. B., Nestola, F., Bullock, E. S., Wang, J. H., Richardson, S. H., & Wang, W. Y. (2016). Large gem diamonds from metallic liquid in Earth's deep mantle. *Science*, *354*(6318), 1403–1405. https://doi.org/10.1126/science.aal1303

Smyth, J. R., & Ahrens, T. J. (1997). The crystal structure of calcite III. *Geophysical Research Letters*, *24*(13), 1595–1598. https://doi.org/10.1029/97GL01603

Stagno, V., Frost, D. J., McCammon, C. A., Mohseni, H., & Fei, Y. (2015). The oxygen fugacity at which graphite or diamond forms from carbonated bearing melts in ecologitic rocks. *Contributions to Mineralogy and Petrology*, *169*(2), 16. https://doi.org/10.1007/s00410-00015-01111-00411

Suito, K., Namba, J., Horikawa, T., Taniguchi, Y., Sakurai, N., Kobayashi, M., et al. (2001). Phase relations of $CaCO_3$ at high pressure and high temperature. *American Mineralogist*, *86*(9), 997–1002. https://doi.org/10.2138/am-2001-8-906

Thomson, A. R., Walter, M. J., Kohn, S. C., & Brooker, R. A. (2016). Slab melting as a barrier to deep carbon subduction. *Nature*, *529*(7584), 76–79. https://doi.org/10.1038/nature16174

Toby, B. H. (2001). EXPGUI, a graphical user interface for GSAS. *Journal of Applied Crystallography*, *34*(2), 210–213. https://doi.org/10.1107/S0021889801002242

Walter, M. J., Bulanova, G. P., Armstrong, L. S., Keshav, S., Blundy, J. D., Gudfinnsson, G., et al. (2008). Primary carbonatite melt from deeply subducted oceanic crust. *Nature*, *454*(7204), 622–625. https://doi.org/10.1038/nature07132

Wirth, R., Kaminsky, F., Matsyuk, S., & Schreiber, A. (2009). Unusual micro- and nano-inclusions in diamonds from the Juina Area, Brazil. *Earth and Planetary Science Letters*, *286*(1-2), 292–303. https://doi.org/10.1016/j.epsl.2009.06.043